elements modeling are demonstrated and there is a good agreement between full wave simulation and small dipole formulas, so the validity of the design method is confirmed by measurement finally.

REFERENCES

1. J.T. Aberle, et al., Reconfigurable antennas for wireless devices, IEEE Antennas Propagat Mag 45 (2003), 148–154.
2. N. Behdad and K. Sarabandi, Dual-band reconfigurable antenna with a very wide tunability range, IEEE Antennas Propagat Trans 54 (2006), 409–416.
3. A.C. Mak, et al., Reconfigurable multiband antenna designs for wireless communication devices, IEEE Trans Antennas Propagat 55 (2007), 1919–1928.
4. D.E. Anagnostou and A.A. Gheethan, A coplanar reconfigurable folded slot antenna without bias network for WLAN applications, IEEE Antennas Wireless Propag Lett 8 (2009), 1057–1060.
5. J.-H. Lim, et al., A reconfigurable PIFA using a switchable PIN-diode and a fine-tuning varactor for USPCS/WCDMA/m-WiMAX/WLAN, IEEE Trans Antennas Propag 58 (2010), 2404–2411.
6. J.S. Petko and D.H. Werner, Miniature reconfigurable three-dimensional fractal tree antennas, IEEE Trans Antennas Propag 52 (2004), 1945–1956.
7. S.A. Schelkunoff and H.T. Friis, Antennas: Theory and practice, vol. 639, Wiley, New York, 1952.

A COMPACT PRINTED TRIANGULAR MONOPOLE ANTENNA FOR ULTRAWIDEBAND APPLICATIONS

Murli Manohar, Rakhesh S. Kshetrimayum, and Anup K. Gogoi
Department of Electronics and Electrical Engineering, Indian Institute of Technology Guwahati, Guwahati 781039, Assam, India; Corresponding author: m.manohar@iitg.ernet.in

Received 2 September 2013

ABSTRACT: *In this article, a printed triangular-shaped monopole antenna is proposed for emerging ultrawideband application. The proposed antenna uses a triangular radiating patch which is directly fed by a 50-Ω microstrip feed line. To improve the impedance bandwidth, a round-corner ground plane has been used. To further improve the impedance bandwidth for the entire band, a microstrip transition (near the antenna front end) has been introduced between the microstrip feed line and the triangular radiator that provides a wide impedance bandwidth from 1.8 to 15.0 GHz for* $|S_{11}| \leq -10$ *dB. The proposed antenna has been realized using the FR-4 printed circuit board substrate and occupies a small size of about* $24 \times 30 \times 1.6$ *mm*^{3} *compared to conventional antenna structures. The proposed antenna has nearly omnidirectional radiation pattern and moderate gain throughout the operating frequency region.* © 2014 Wiley Periodicals, Inc. Microwave Opt Technol Lett 56:1155–1159, 2014; View this article online at wileyonlinelibrary.com. DOI 10.1002/mop.28290

Key words: *printed monopole antenna; ultrawideband; antenna time and frequency domain characteristics*

1. INTRODUCTION

Currently there is a great attention paid for ultrawideband (UWB) systems since Federal Communication Commission (FCC) has announced in 2002the unlicensed use of the 3.1–10.6 GHz band with equivalent isotropic radiation power (EIRP) less than −41.3 dBm/MHz for commercial UWB communication applications [1]. Due to numerous features, such as high-speed data rate, low power consumption, small emission power, and low cost, UWB system has gained much attraction in the recent years. Some applications of UWB systems are personal area network, radar imaging systems, ground-penetrating radar, and biomedical imaging, respectively [2,3].

Printed monopole antennas are currently under consideration for use in emerging UWB application as they exhibit very attractive merits such as broadband impedance matching, compact size, and omni-directional radiation pattern. Many techniques have been examined to improve the antenna bandwidth in the past few years. Low et al. [4] described enhancement of impedance bandwidth of the planar monopole by suspended plate antenna. Ammann [5] discussed control of the impedance bandwidth of wideband planar monopole antennas using a beveling technique. Jung et al. [6] discussed a compact and low-profile wideband antenna with an L-shaped notch. Wi et al. [7] achieved wideband characteristics using U-shaped microstrip parasitic elements. Oraizi and Hedayati [8] carried out a combination of GiusepePeano and Sierpinski Carpet fractals shaped for wideband impedance matching. As is well known, UWB antennas with various shapes such as cone shaped [9], triangular shaped [10], circular shaped [11], fork shaped [12], elliptical shaped [13], and inverted-F shaped [14] were reported in literature. However, small size and wide bandwidth is essentially required for UWB applications. Size miniaturization as well as ultrawide bandwidth of UWB monopole antenna is a challenging task for modern multipurpose handheld devices. In this communication, a novel printed triangular monopole antenna (PTMA) with enhanced bandwidth is proposed for UWB applications. The proposed antenna structure has wide bandwidth and is small in size compared to the antenna dimensions reported in [10–15]. The impedance bandwidth of the proposed triangular monopole antenna is greatly improved by introducing a transition between the microstrip feed line and the printed triangular patch with the round-corner ground plane. The antennas were simulated using frequency domain 3D full wave electromagnetic solver (HFSS version 14).

2. ANTENNA GEOMETRY AND DESIGN

The geometry of the proposed triangular monopole antenna is shown in Figure 1. In this communication, a novel 50-Ω microstrip transition feed line fed UWB PTMA with a round-corner ground plane is proposed. The proposed antenna consists of a triangular-shaped radiator on the top connected with a 50-Ω microstrip transition feed line and the round-corner ground plane is printed on the backside of FR4-substrate as shown in Figure 1. The antenna is printed on a 1.6-mm-thick FR4-substrate with a dielectric constant of 4.4 and a loss tangent of 0.018. The proposed antenna structure occupies overall dimension of about $24 \times 30 \times 1.6$ mm^3. The detailed dimensions of the proposed antenna are given in Table 1. Figure 2 shows the impedance bandwidth improvement process of the monopole antenna. Generally, a simple triangular patch antenna has narrow-band characteristics. To improve impedance bandwidth in this antenna, we shape the partially etched rectangular ground plane of the Antenna 1 into round-corner ground plane (denoted as Antenna 2). To further improve the impedance matching for the entire band, a microstrip transition is introduced (near the front end of the radiating patch) between the 50-Ω microstrip feed line and the printed triangular patch (denoted as Antenna 3). Because of this transition involves stepped changes in impedance function

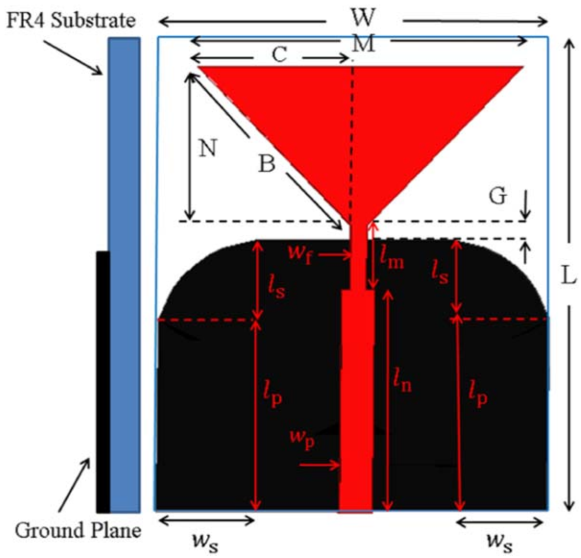

Figure 1 Geometry of the proposed triangular monopole antenna. [Color figure can be viewed in the online issue, which is available at wileyonlinelibrary.com]

(i.e., a single-section transformer), it increases the bandwidth of the transformer as antenna impedance becomes closer to the characteristic impedance of the microstrip feed line. The proposed antenna starts resonating from 1.8 GHz, as the resonant path ($C + B + G$) of the triangular monopole is close to quarter wavelength at this frequency. The lowest frequency within the bandwidth of the antenna can be calculated using three parameters C, B, and G, which is given by

$$f_L = \frac{v_0}{4(C+B+G)\sqrt{\varepsilon_{eff}}} \quad (1)$$

where v_0 is the speed of light and ε_{eff} is the effective dielectric constant of the substrate.

3. PARAMETRIC STUDY

Figure 3 shows comparison of the simulated reflection coefficient of Antenna 1, Antenna 2, and Antenna 3. It can be observed that by introducing an impedance step between microstrip feed line and radiating patch, the bandwidth of the proposed antenna increases from 111.1 to 157.1%. The simulated reflection coefficient of the UWB antenna with different values of l_m is shown in Figure 4. It is clearly seen that as l_m decreases from 4 to 2 mm, the impedance matching of the monopole antenna is gradually affected at resonant frequencies around 8 and 13.5 GHz. However, as l_m increases from 4 to 5 mm, improvement of the impedance bandwidth within the UWB frequency region, but there is impedance mismatch from frequency band between 12 and 14 GHz. So, the optimal value of this parameter for maximum impedance bandwidth is 4 mm.

Figure 5 demonstrates the simulated reflection coefficient of the proposed PTMA for the various patch length N. The length N of the triangular patch determines the resonant frequency. It is observed that the impedance bandwidth is the widest as the dimension of patch length N increase from 6 to 10 mm, whereas by decreasing the patch length N, the lower frequency is shifted toward right, which results in decreased percentage bandwidth. At $N = 10$, the lowest resonant frequency moves toward lower frequency and gives wide bandwidth with minimum impedance mismatch. Thus, the impedance bandwidth of the optimized UWB monopole antenna can be enhanced by selecting the suitable value of $N = 10$.

Figure 6 illustrates the simulated reflection coefficient curves with the different size of the overall round-corner ground plane. As the size of the ground plane structure decreases from 17 × 24 to 16 × 23 mm^2, the reflection coefficient is greater than −10 dB only at 5 GHz. Furthermore, when the size of the ground plane structure again decreases from 16 × 23 to 15 × 22 mm^2, magnitude of reflection coefficient tends to be >–10 dB within the UWB frequency region. It shows that the impedance matching gradually becomes worse, when the size of the ground plane structure decreases.

TABLE 1 Dimensions of the Proposed UWB Triangular Monopole Antenna

Parameters	L	W	W_S	W_P	W_f	l_m	l_s	l_n	l_p	N	B	G	M	C
Units (mm)	30	24	6	2	1	4	5	14	12	10	13.8	1	20	9.5

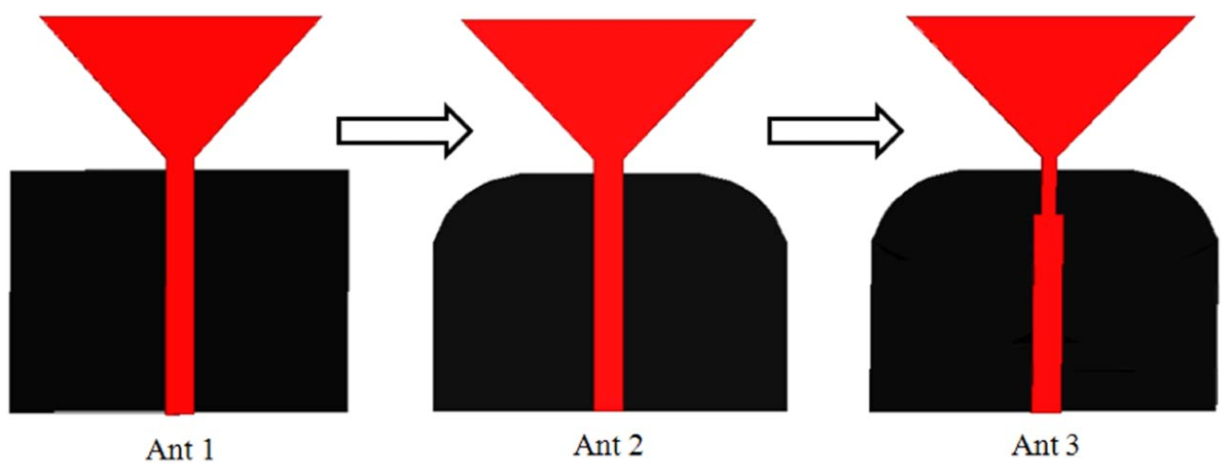

Figure 2 Impedance bandwidth improvement process. [Color figure can be viewed in the online issue, which is available at wileyonlinelibrary.com]

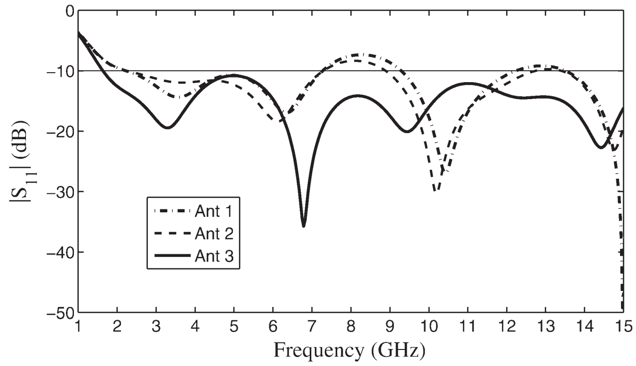

Figure 3 Simulated reflection coefficient of Antenna 1, Antenna 2, and Antenna 3

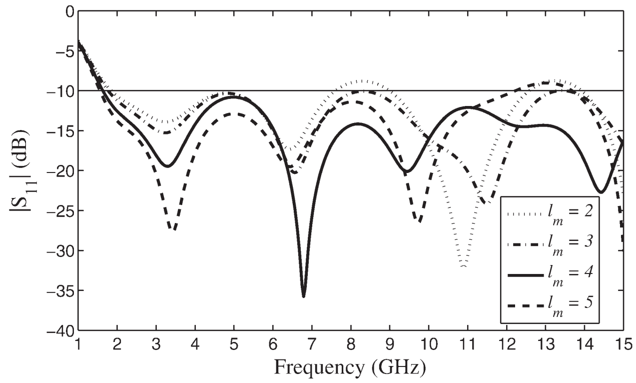

Figure 4 Parametric studies on effect of different values of on return loss of the proposed antenna

Thus, better impedance matching is achieved with a size of the ground plane structure of 17×24 mm^2. We can observe that the Antenna 3 gives broader bandwidth than Antenna 1 and Antenna 2.

4. EXPERIMENTAL RESULTS

A picture of the fabricated UWB PTMA is shown in Figure 7. The measurement of triangular monopole antenna was done by

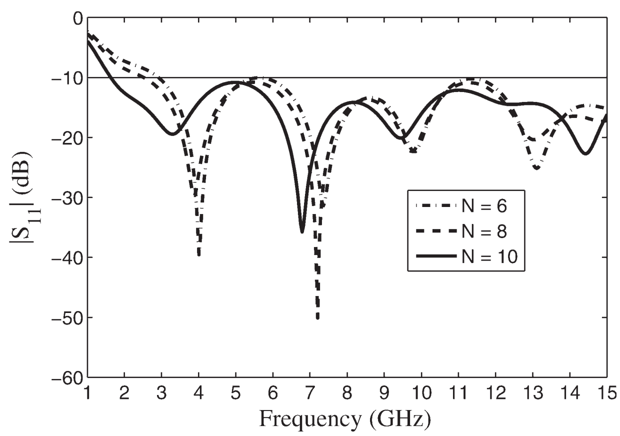

Figure 5 Parametric studies on effect of various patch length *N* on return loss of the proposed antenna

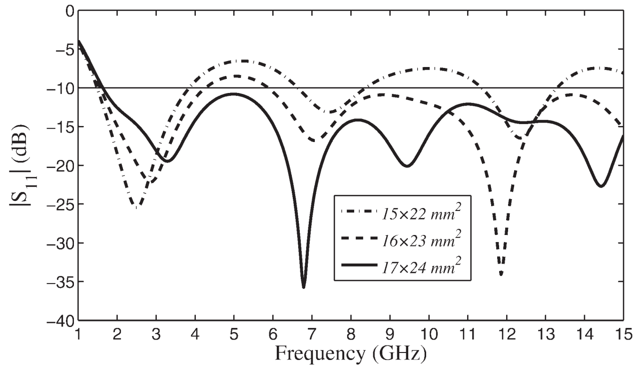

Figure 6 Simulated reflection coefficient curves with the different size of the overall round-corner ground plane

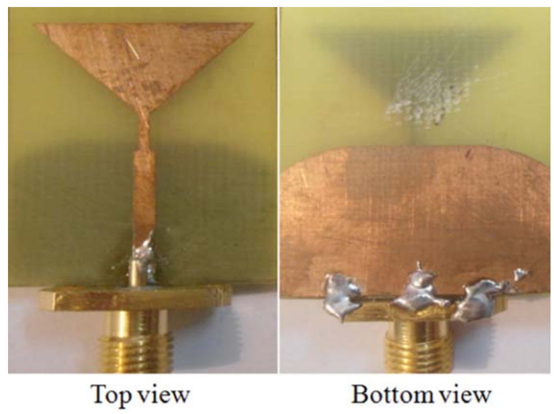

Figure 7 Photograph of the fabricated printed triangular UWB monopole antenna. [Color figure can be viewed in the online issue, which is available at wileyonlinelibrary.com]

Rohde and Schwarz ZVA24 vector network analyzer. Figure 8 plots the measured and simulated return loss as a function of frequency. There is reasonably good agreement between simulation and measurement results throughout the UWB frequency region. Figures 9(a)–9(c) shows the measured radiation patterns in the *E*- and *H*-plane at frequencies 3.1, 7.0, and 10.0 GHz, respectively. The *E*-plane radiation pattern shows a typical figure-of-eight at frequencies of 3.1, 7.0, and 10.0 GHz, which

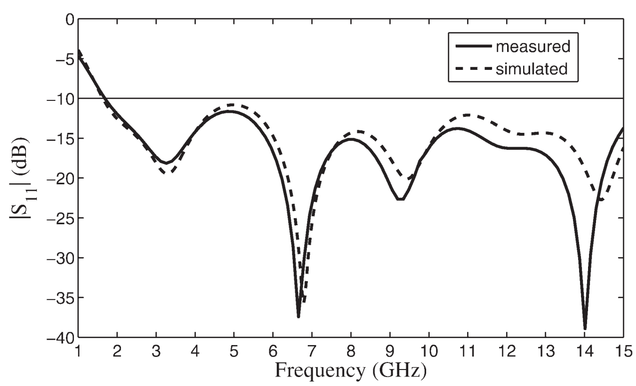

Figure 8 Measured and simulated return loss for the proposed triangular UWB monopole antenna

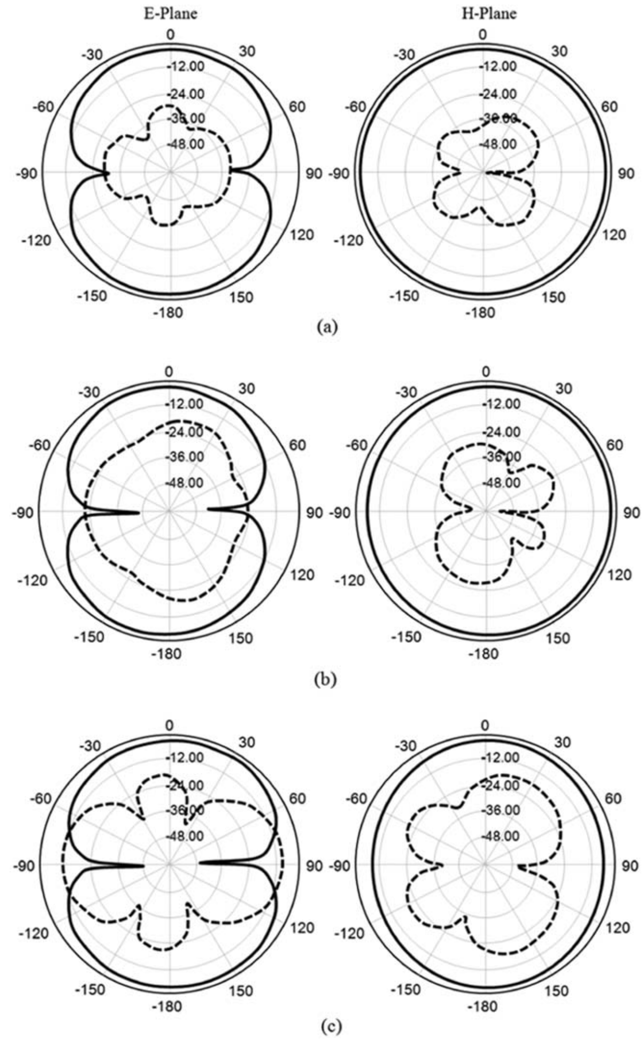

Figure 9 Measured radiation pattern for the proposed triangular UWB monopole antenna at (a) 3.1 GHz, (b) 7.0 GHz, and (c) 10.0 GHz

shows that this antenna behaves like a conventional dipole or biconical antenna. A low cross polarization was observed within the FCC suggested UWB frequency region. It can be observed that the antenna has nearly omni-directional radiation pattern at frequencies of 3.1, 7.0, and 10.0 GHz in the

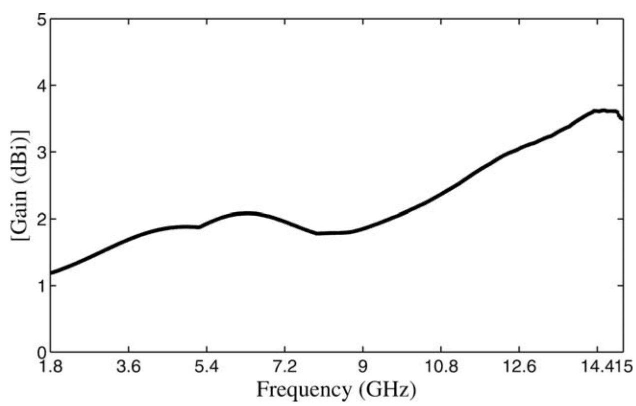

Figure 10 Measured gain for the proposed triangular UWB monopole antenna

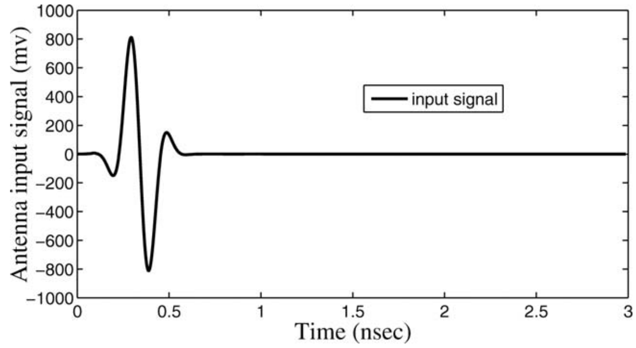

Figure 11 Fifth derivative of Gaussian pulse waveform in time domain

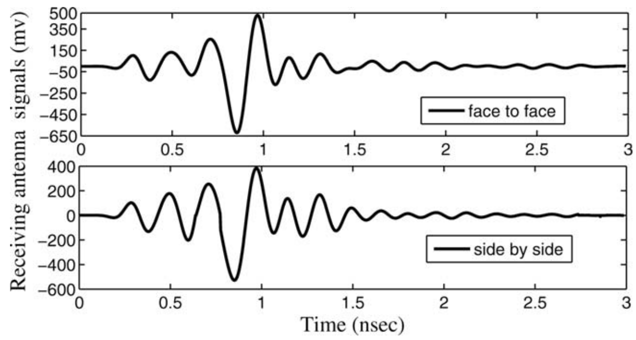

Figure 12 Face-to-face and side-by-side received pulse in time domain for an UWB system with two identical antennas

H-planes. Figure 10 plots the measured peak gain over the operating frequency from 1.8 to 15.0 GHz. It can be seen that the peak gain for the triangular monopole antenna is about 3.7 dBi. To analyze the signal dispersion in the UWB system, a time domain characteristic has been investigated. In this scheme, two identical antennas are kept at a distance of 60 cm in face-to-face and side-by-side. A fifth derivative Gaussian pulse, as presented in (2), is used as the source signal to drive the transmitter [16].

$$G_5(t)=A\left(-\frac{t^5}{\sqrt{2\pi}\sigma^{11}}+\frac{10t^3}{\sqrt{2\pi}\sigma^9}-\frac{15t}{\sqrt{2\pi}\sigma^7}\right).\exp\left(-\frac{t^2}{2\sigma^2}\right) \quad (2)$$

where A is a constant chosen to meet the limitation set by FCC and σ has to be 51 ps to satisfy the FCC limitation. Figure 11 shows the fifth-order derivative of Gaussian pulse waveform

TABLE 2 Comparison of the Size and Bandwidth of the Proposed Triangular Monopole Antenna to Conventional Antennas

Antenna Structures	Dimensions ($L \times W \times h$) (mm^3)	Freq. Range (GHz) and BW (GHz)
Cone shape [9]	76.2 × 76.2 × 0.79	1–10, 9
Triangular shaped [10]	60 × 20 × 1	4–10, 6
Circular shaped [11]	50 × 42 × 1.5	2.78–9.78, 7
Fork shape [12]	42 × 24 × 1.6	3.1–12, 8.9
Elliptical shaped [13]	45 × 45 × 1.57	3–14, 11
Inverted-F shaped [14]	50 × 30 × 2	2–6, 4
Proposed triangular shape	30 × 24 × 1.6	1.8–15, 13.2

with a width of 300 ps in the time domain. The fifth-order Gaussian pulse is generated in Tektronix AWG 7122B arbitrary signal generator and it is fed to the UWB antenna. At the receiver, the signal received by the UWB antenna is captured in Tektronix DPO 70804 digital phosphor oscilloscope. The input and received waveforms for the face-to-face and side-by-side orientations of the antenna are shown in Figure 12. It can be observed that there is minimum dispersion in side-by-side received signal as compare to face-to-face received signal.

5. CONCLUSION

In this article, a PTMA fed by microstrip feed line is proposed and investigated. It gives a broad measured bandwidth from 1.8 to 15.0 GHz. To enhance the bandwidth, a single-section impedance transformer and a round-corner partially etched ground plane has been used. The proposed antenna structure has wide bandwidth and small size compared to the conventional antenna (refer to Table 2). The measured antenna radiation patterns show omni-directional characteristics. The measured gain variation within the bandwidth is less than 2.6 dBi approximately.

REFERENCES

1. FCC, Ultra-wideband operation FCC report and order, Technical Report US 47 CFR Part15, Washington, DC, 2002.
2. WPAN high rate alternative PHY task group 3a (TG3a), IEEE 802.15. Available: http://ieee802.org/15/pub/TG3a.html.
3. D.W. Winters, J.D. Shea, E.L. Madsen, G.R. Frank, B.D. Van Veen, and S.C. Hagness, Estimating the breast surface using UWB microwave monostatic backscatter measurements, IEEE Trans Biomed Eng 55 (2008), 247–256.
4. X.N. Low, Z.N. Chen, and W.K. Toh, Ultrawideband suspended plate antenna with enhance impedance and radiation performance, IEEE Trans Antennas Propag 56 (2008), 2490–2495.
5. M. Ammann, Control of the impedance bandwidth of wideband planar monopole antennas using a beveling technique, Microwave Opt Technol Lett 30 (2004), 229–232.
6. J. Jung, W. Choi, and J. Choi, A compact broadband antenna with an L-shaped notch, IEICE Trans Commun E89-B (2006), 1968–1971.
7. S.H. Wi, Y.-S. Lee, and J.-G. Yook, Wideband microstrip patch antenna with U-shaped parasitic elements, IEEE Trans Antennas Propag 55 (2007), 1196–1199.
8. H. Oraizi and S. Hedayati, Miniaturized UWB monopole microstrip antenna design by the combination of GiusepePeano and Sierpinski carpet fractals, IEEE Antennas Wireless Propag Lett 10 (2011), 67–70.
9. S.Y. Suh, W. Stutzman, and W. Davis, A new ultrawideband printed monopole antenna: The planar inverted cone antenna (PICA), IEEE Trans Antennas Propag 52 (2004), 1361–1364.
10. C.C. Lin, Y.C. Kan, L.C. Kuo, and H.R. Chuang, A planar triangular monopole antenna for UWB communication, IEEE Microwave Wireless Compon Lett 15 (2005), 624–626.
11. J. Liang, C. Chiau, X. Chen, and C. Parini, Printed circular disc monopole antenna for ultra-wideband applications, Electron Lett 40 (2004), 1246–1247.
12. S.K. Mishra, R.K. Gupta, A. Vaidya, and J. Mukherjee, A compact dual-band fork-shaped monopole antenna for bluetooth and UWB applications, IEEE Antennas Wireless Propag Lett 10 (2011), 627–630.
13. A. Elboushi, O.M. Ahmed, and A.R. Sebak, Study of ellpitical slot UWB antennas with a 5.0–6.0 GHz band-notch capability, Prog Electromagn Res C 16 (2010), 207–222.
14. M.Y. Man, R. Yang, Z.Y. Lei, Y.J. Xies, and J. Fan, Ultra-wideband planar inverted-F antennas with cut-etched ground plane, Electron Lett 48 (2012), 817–818.
15. M.N. Moghadasi, H. Rousta, and B.S. Virdee, Compact UWB planar monopole antenna, IEEE Antennas Wireless Propag Lett 8 (2009), 1382–1385.
16. H. Kim, D. Park, and Y. Joo, All-digital low-power CMOS pulse generator for UWB system, Electron Lett 40 (2004), 1534–1535.

AN X-BAND CMOS POWER AMPLIFIER WITH A DRIVER STAGE USING A SHOT-THROUGH CURRENT REJECTION TECHNIQUE

Jonghoon Park and Changkun Park
School of Electronic Engineering, College of Information Technology, Soongsil University, 551 Sangdo-Dong, Dongjak-Gu, Seoul 156-743, Republic of Korea; Corresponding author: pck77@ssu.ac.kr

Received 3 September 2013

ABSTRACT: *In this study, we design an X-band switching-mode CMOS power amplifier using 0.13-μm RF CMOS process. The power amplifier is composed of driver and power stages. In this study, we focus on the power consumption of the driver stage. To minimize power consumption, we propose a shot-through current rejection technique for the Class-D amplifier used as a driver stage of the CMOS power amplifier. We split the gate bias of the NMOS and PMOS of the Class-D amplifier using DC-blocking capacitors to control the shot-through current. From the measured results, we successfully prove the feasibility of the proposed technique.* © 2014 Wiley Periodicals, Inc. Microwave Opt Technol Lett 56:1159–1162, 2014; View this article online at wileyonlinelibrary.com. DOI 10.1002/mop.28289

Key words: *Class-D; driver stage; efficiency; gate bias; power amplifier; shot-through current*

1. INTRODUCTION

Power amplifiers have many uses owing to their essential functions for wireless communication systems [1–3]. In particular, along with the requirement of low-cost implementation, power amplifiers that use CMOS technology have become more popular [4–7]. However, CMOS power amplifiers present lower efficiency compared to amplifiers designed using III–V compound semiconductors. Although there have been many earlier attempts to enhance the efficiency of CMOS power amplifiers, most previous works have focused on a reduction of the loss induced by the power stages to improve the overall efficiency. For example, to overcome the low efficiency of CMOS power amplifiers, multi-mode and feedback architectures have been reported [8–11].

In this study, we focus on the power consumption of the driver stage of switching-mode RF CMOS power amplifiers. First, to identify the problems that degrade the entire efficiency of switching-mode CMOS power amplifiers, we investigate the Class-D type driver stages of the power amplifiers in terms of the shot-through current. To solve the problems found for the Class-D type driver stage, we propose a shot-through current rejection technique for the Class-D type driver stage.

2. TYPICAL CLASS-D TYPE DRIVER STAGE

Generally, power amplifiers are designed using a multistage structure to guarantee required gain specification, as shown in Figure 1. If the designed power amplifier is in switching mode, a driver stage supports the transistors of the power stage to operate as switch while the power stage generates high output power. One well-